Inorg. Chem. **2008**, *47*, 6001−6008

Structure of Fe/Co/Ni Hexacyanoferrate As Probed by Multiple Edge X-ray Absorption Spectroscopy

Marco Giorgetti* and Mario Berrettoni

Dipartimento di Chimica Fisica ed Inorganica, Alma Mater Studiorum, Università di Bologna and Unità di Ricerca INSTM di Bologna, Viale Risorgimento 4, 40136 Bologna, Italy

Received February 14, 2008

The structural parameters in selected cobalt and mixed cobalt/nickel hexacyanoferrates have been determined by X-ray absorption spectroscopy. The presence of two or three metals in the sample requires the use of a highly efficient multiple edge analysis. The typical structure of mixed hexacyanoferrates coupled with a suitable data analysis program, GNXAS, allow us to determine structural parameters considering a very high number of experimental points. The first data analysis of three contiguous edges (Fe, Co, and Ni K-edges), the structural parameters of which are entirely correlated, is presented. The advantages and limitations of the multiple edge approach are underlined and placed in the context of the previous studies. The CN bond length has been determined with a statistical error of few thousandths of an angstrom.

Introduction

A key features of the X-ray Absorption Fine Structure (XAFS) technique is the possibility of determining the local atomic environment of a selected atomic specie, in a range limited by the photoelectron mean free path, simply by tuning the energy of the incoming beam around its K-edge. In the past decades, XAFS has been proved to be a strong structural tool,[1–6] capable of carrying structural studies on amorphous and disordered materials,[3,4] inorganic materials,[7] biological materials,[8,9] solutions,[10] and also including *in situ* techniques.[9,11]

In the case of a multicomponent system where a second atomic specie is present, XAFS probe could be tuned to the two local atomic environments. Data analysis is carried out on both experimental XAFS signals and the local structure is revealed. Otherwise, data analysis could be done simultaneously on the two edges. This approach, called multiple-edge structural refinement,[12] has been first applied to the study of the L edges (L_I, L_{II}, and L_{III}) in liquid and crystalline Sn, producing interesting results. Afterward, the method has been extended to the analysis of K-edges by Hogdson et al.[13,14] by studying the iron−copper bridged in molecular assemblies and further applied by Di Cicco et al. to study the short-range order of binary alloys[15–17] in both solid and liquid state. In addition, Weller et al. reported[18] on combined K-edges X-ray absorption spectroscopy (XAS) and power

* To whom correspondence should be addressed. E-mail: marco.giorgetti@unibo.it. Phone: +39 051 209 3666. Fax: +39 051 209 3690.

(1) Sayers, D. E.; Stern, E. A.; Lytle, F. W. *Phys. Rev. Lett.* **1971**, *27*, 1204.
(2) Lee, P. A.; Citrin, P. H.; Eisenberger, P.; Kincaid, B. M. *Rev. Mod. Phys.* **1981**, *53*, 769.
(3) Filipponi, A. *J. Phys.: Condens. Matter* **2001**, *13*, R23.
(4) Giorgetti, M.; Berrettoni, M.; Scaccia, S.; Passerini, S. *Inorg. Chem.* **2006**, *45*, 2750.
(5) Giorgetti, M.; Berrettoni, M.; Smyrl, W. H. *Chem. Mater.* **2007**, *19*, 5991.
(6) Rehr, J. J.; Albers, R. C. *Rev. Mod. Phys.* **2000**, *72*, 621.
(7) Solomon, E. I.; Hedman, B.; Hogdson, K. O.; Dey, A.; Szilagyi, R. K. *Coord. Chem. Rev.* **2005**, *249*, 97.
(8) Levina, A.; Armstrong, R. S.; Lay, P. A. *Coord. Chem. Rev.* **2005**, *249*, 141.
(9) Giorgetti, M.; Ascone, I.; Berrettoni, M.; Conti, P.; Zamponi, S.; Marassi, R. *J. Biol. Inorg. Chem.* **2000**, *5*, 156.
(10) D'Angelo, P.; Benfatto, M.; Della Longa, S.; Pavel, N. V. *Phys. Rev. B* **2002**, *66*, 064209.
(11) Giorgetti, M.; Passerini, S.; Smyrl, W. H.; Muckerjee, S.; Yang, X. Q.; McBreen, J. *J. Electrochem. Soc.* **1999**, *146*, 2387.
(12) Di Cicco, A. *Phys. Rev. B.* **1996**, *53*, 6174.
(13) Zhang, H. H.; Filipponi, A.; Di Cicco, A.; Scott, M. J.; Holm, R. H.; Hedman, B.; Hogdson, K. O. *J. Am. Chem. Soc.* **1997**, *119*, 2470.
(14) Zhang, H. H.; Filipponi, A.; Di Cicco, A.; Lee, S. C.; Scott, M. J.; Holm, R. H.; Hedman, B.; Hogdson, K. O. *Inorg. Chem.* **1996**, *35*, 4819.
(15) Minicucci, M.; Di Cicco, A. *Phys. Rev. B.* **1997**, *56*, 11456.
(16) Di Cicco, A.; Taglienti, M.; Minicucci, M.; Filipponi, A. *Phys. Rev. B.* **2000**, *62*, 12001.
(17) Trapananti, A.; Di Cicco, A.; Minicucci, M. *Phys. Rev. B.* **2002**, *66*, 014202.
(18) Weller, M. T.; Pack, M. P.; Binsted, N. *Angew. Chem., Int. Ed.* **1998**, *37*, 1094.

10.1021/ic800289c CCC: $40.75
Published on Web 06/11/2008

X-ray diffraction (XRD) data refining using a shared set of coordinates.

This paper presents the structural characterization of cobalt and mixed cobalt/nickel hexacyanoferrates[19–21] using a multiple edge approach. The present XAFS data analysis on metal hexacyanoferrates upgrades the former ones[22–24] which have been carried out considering single-edge approaches. This class of compound belongs to Prussian Blue (PB) compounds, a pigment used since the 18th century. In the past decade, the renewed attention to these materials is based on their use as magnetic devices. In particular, the discovery of the photoinduced magnetization effects in some hexacyanoferrate compounds[25–28] has been addressed. Besides, different routes of synthesis have been pursued.[29–31] In addition, typical properties of these materials are electrochromism,[19,21,32] electrocatalysis,[33] ion-sieving membranes,[34] charge storage,[35] diffusion properties,[36] corrosion protection,[37] and analytical sensing.[38–41]

From the structural viewpoint, these complexes are characterized by a rigid three-dimensional cubic network (although other crystal symmetries are found in a few other hexacyanoferrates) of repeating −NC−Ma−CN−Mb−NC− units where Ma is Fe and Mb is Co and/or Ni. Iron and cobalt sites are typically octahedral, and the sites at the cube center are occupied by water as well as countercations as necessary to achieve charge neutrality. Hence, the peculiarity of this structures of being formed by an almost perfect linear atomic chains; a high degeneration of the atomic chains (six) and a short distance between Mb and Ma (about 5 Å) allowed the cobalt hexacyanoferrate to be used as prototype for a four body Multiple Scattering XAFS calculation.[42,43] Furthermore, the peculiar structure of metal hexacyanoferrate permits one to study the entire molecular complex by analyzing Fe, Co, and Ni edges simultaneously. In this case, common structural units share the same set of parameters. Although multiple edge approaches using some correlated parameters have been reported in the literature,[13,14] this data analysis involves three contiguous metals K-edges which are entirely structurally correlated, that is, no additional parameters are needed to be included in the fitting approach that are exclusive for explaining the other metal K-edge. This is due to the symmetry of this structure. Strengths and limitations of the multiple edge approach in this class of compounds is presented, and the quotation of the bond length between carbon and nitrogen is given.

Table 1. List of the Investigated Compounds and Their Stoichiometry[a]

	ratio Ni:Co:Fe	
compounds (formal stoichiometry)	EDXF	by XAS
(**I**) $Na_2Co^{II}Fe^{II}(CN)_6$	0:1.09:1	0:1.18:1.00
(**II**) $NaCo^{II}Fe^{III}(CN)_6$	0:1.36:1	0:1.59:1
(**III**) $KNi^{II}Co^{II}Fe^{II}(CN)_6$	0.65:0.52:1	0.63:0.59:1.00

[a] Please note that the error bars on the XAS ratio determination is in the order of one decimal place (see text).

Experimental Section

Sample Preparation. Solid samples of mixed hexacyanoferrates were prepared following the preparation described in ref 9. All chemicals were reagent grade and were used as received. All solutions were prepared using freshly prepared doubly distilled water. The samples considered in the present paper are $Na_2Co^{II}Fe^{II}(CN)_6$ (**I**), $NaCo^{II}Fe^{III}(CN)_6$ (**II**), and $KNi^{II}Co^{II}Fe^{II}(CN)_6$ (**III**).

Chemical Analysis. The chemical composition of compounds has been determined by energy dispersive X-ray fluorescence analysis (courtesy by Analisi Control Laboratory, Corridonia, Italy). This method was preferred because the analysis can be done on pellets of powder sample avoiding the dissolution step needed in the more common AAS. Table 1 displays the results.

XRD. The XRD pattern was recorded on powder samples. Data were collected at a Philips diffractometer, X-ray source PW1830 and PW 1050/37 goniometer, using Cu Kα radiation, in the 2θ interval 3−70°, a 0.02° step, and with an integration time of 3 s. The XRD data are refined to calculate the cell parameters a with the free-available program Unit Cell developed by T.J.B. Holland and S.A.T. Redfern (1997).

XAS Data Collection. XAS experiments were performed at room temperature at the Synchrotron Radiation Source (SRS) at Daresbury Laboratory, Warrington, England using the beam line 7.1. The storage ring operates at 1.6 GeV with a typical current of 240 mA. A Si (111) double crystal monochromator was employed. To reduce higher harmonics, the second crystal was detuned at about 70%. Internal references for energy calibration were used for iron, cobalt, and nickel. Data at the Fe, Co, and Ni K-edge were acquired

(19) Kulesza, P. J.; Malik, M. A.; Berrettoni, M.; Giorgetti, M.; Zamponi, S.; Schmidt, R.; Marassi, R. *J. Phys. Chem. B* **1998**, *102*, 1870.
(20) Lezna, R. O.; Romagnoli, R.; de Tacconi, N. R.; Rajeshwar, K. *J. Phys. Chem. B* **2002**, *106*, 3612.
(21) Kulesza, P. J.; Malik, M. A.; Skorek, J.; Miecznikowski, K.; Zamponi, S.; Berrettoni, M.; Giorgetti, M.; Marassi, R. *J. Electrochem. Soc.* **1999**, *146*, 3757.
(22) Yokoyama, T.; Otha, T.; Sato, O.; Hashimoto, K. *Phys. Rev. B* **1998**, *58*, 8257.
(23) Yokoyama, T.; Kiguchi, M.; Otha, T.; Sato, O.; Einaga, Y.; Hashimoto, K. *Phys. Rev. B* **1999**, *60*, 9340.
(24) Cartierdit, C.; Moulin, Villain, F.; Bleuzen, A.; Arrio, M. A.; Sainctavit, P.; Lomenech, C.; Escax, V.; Baudelet, F.; Dartyge, E.; Gallet, J. J.; Verdaguer, M. *J. Am. Chem. Soc.* **2000**, *122*, 6653.
(25) Sato, O.; Iyoda, T.; Fujishima, A.; Hashimoto, K. *Science* **1996**, *272*, 704.
(26) Sato, O. *Acc. Chem. Res.* **2003**, *36*, 692.
(27) Ferlay, S.; Mallah, T.; Ouahes, R.; Veillet, P.; Verdaguer, M. *Science* **1996**, *271*, 49.
(28) Bleuzen, A.; Lomenech, C.; Escax, V.; Villain, F.; Varret, F.; Cartier dit Moulin, Ch.; Verdaguer, M. *J. Am. Chem. Soc.* **2000**, *122*, 6648.
(29) Carpani, I.; Giorgetti, M.; Berrettoni, M.; Buldini, P. L.; Gazzano, M.; Tonelli, D. *J. Solid State Chem.* **2006**, *179*, 3981.
(30) Carpani, I.; Berrettoni, M.; Giorgetti, M.; Tonelli, D. *J. Phys. Chem. B* **2006**, *110*, 7265.
(31) Giorgetti, M.; Berrettoni, M.; Zamponi, S.; Kulesza, P. J.; Cox, J. A. *Electrochim. Acta* **2005**, *51*, 511.
(32) Monk, P. M. S.; Mortimer, R. L.; Rosseinsky, D. R. *Electrochromism, Fundamental and Applications*; VCH: Weinheim, 1995.
(33) Zhou, D. M.; Ju, H. X.; Chen, X. Y. *J. Electroanal. Chem.* **1998**, *408*, 219.
(34) Pyrasch, M.; Toutianoush, A.; Jin, W. Q.; Schnepf, J.; Tieke, B. *Chem. Mater.* **2003**, *15*, 245.
(35) Neff, V. D. *J. Electrochem. Soc.* **1985**, *132*, 1382.
(36) Kahlert, H.; Retter, U.; Lohse, H.; Siegler, K.; Scholz, F. *J. Phys. Chem. B* **1998**, *102*, 8757.
(37) Deng, Z.; Smyrl, W. H. *J. Electrochem. Soc.* **1991**, *138*, 1911.
(38) Scholz, F.; Dostal, A. *Angew. Chem., Int. Ed. Engl.* **1995**, *34*, 2685.
(39) Coon, D. R.; Amos, L. J.; Bocarsly, A. B. *Anal. Chem.* **1998**, *70*, 3137.
(40) Giorgetti, M.; Scavetta, E.; Berrettoni, M.; Tonelli, D. *Analyst* **2001**, *126*, 2168.
(41) Karyakin, A. A.; Kotel'nikova, E. A.; Lukachova, L. V.; Karyakina, E. E. *Anal. Chem.* **2002**, *74*, 1597.
(42) Giorgetti, M.; Berrettoni, M.; Filipponi, A.; Kulesza, P. J.; Marassi, R. *Chem. Phys. Lett.* **1997**, *275*, 108.
(43) Loeffen, P. W.; Pettifer, R. F. *Phys. Rev. Lett.* **1996**, *76*, 639.

Table 2. Structural Parameters from EXAFS Fitting Results of Samples **I**, **II**, and **III**[a]

	(**I**) $Na_2Co^{II}Fe^{II}(CN)_6$			(**II**) $NaCo^{II}Fe^{III}(CN)_6$			(**III**) $KNi^{II}Co^{II}Fe^{II}(CN)_6$			
	Fe−Co	Fe	Co	Fe−Co	Fe	Co	Fe−Co−Ni	Fe	Co	Ni
Fe−C/Å	1.866(4)	1.864(5)	1.87(1)	1.890(8)	1.885(12)	1.923(15)	1.864(15)	1.865(10)	1.86(2)	1.91(3)
σ^2 Fe−C/Å^2	0.0023(5)	0.0024(5)	0.015(2)	0.0024(10)	0.002(1)	0.015(3)	0.003(2)	0.002(1)	0.025(7)	0.015(7)
CN/Å	1.183(5)	1.192(6)	1.176(10)	1.167(7)	1.178(10)	1.144(8)	1.184(12)	1.20(2)	1.19(2)	1.11(3)
σ^2 C≡N/Å^2	0.009(1)	0.009(2)	0.004(2)	0.013(2)	0.010(3)	0.011(5)	0.005(2)	0.008(3)	0.010(5)	0.003(2)
Co−N/Å	2.100(8)	2.092(15)	2.10(1)	2.095(7)	2.04(3)	2.096(6)	2.09(1)	2.07(3)	2.09(1)	
σ^2 Co−N/Å^2	0.0046(7)	0.007(5)	0.006(1)	0.004(1)	0.007(3)	0.004(2)	0.005(3)	0.009(6)	0.003(2)	
Co−O/Å	2.21(3)		*2.18(3)*	*2.24(2)*		2.22(2)	2.19(6)		2.20(3)	
σ^2 Co−O/Å^2	*0.011(4)*		*0.012(10)*	0.008(3)		0.009(3)	0.017(9)		0.005(4)	
Ni−N/Å							2.07(2)			2.11(2)
σ^2 Ni−N/Å^2							0.007(6)			0.011(3)
Ni−O/Å							2.11(7)			2.02(2)
σ^2 Ni−O/Å^2							0.013(6)			0.002(1)
E_0 (Fe)/eV	7109.5	7109.0		7109.8	7109.6		7110.7	7110.1		
E_0 (Co)/eV	7709.9		7709.4	71012.8		7712.7	7711.9		7711.9	
E_0 (Ni)/eV							8334.3			8334.1
a/2*/Å	5.149	5.148	5.146	5.152	5.103	5.163	5.128**	5.135	5.14	5.13
a (from XRD)		5.14			5.14			5.14		
χ^2-like residual/(10^{-6})	5.19	6.25	4.43	5.45	4.63	10.7	4.18	3.23	16.4	145

[a] The estimated parameter errors are indicated in parentheses. * Data obtained from geometrical consideration using the corresponding three and four body atomic configuration. ** This value is obtained considering a mean value of Co(Ni)-N of 2.08 Å. Data in *italic* (sample **I**) are due to the portion of 'insoluble' structure.

in transmission mode. XAS spectra were recorded using a single optimized scan from 7000 to 9000 eV. This corresponds in the k (Å^{-1}) space to $k = 12$ for each metal K threshold. Data were collected at 0.03 k intervals with a 1 s (start value) to 5 s (final value, at higher k) integration time allowing extended X-ray absorption fine structure (EXAFS) spectra to be recorded sequentially after the near edge X-ray absorption structure (XANES) region. Samples were prepared by mixing powdered compounds with cellulose (Merck) (20:80 w/w) and applying a pressure of about 5 tons cm^{-2} to obtain a pellet.

XAS Data Analysis. XANES spectra were normalized to an edge jump of unity. A prior removal of the background absorption was done by subtraction of a linear function extrapolated from the pre-edge region. The EXAFS analysis was performed using the GNXAS package[44,45] which is based on Multiple Scattering (MS) theory. The method is based on the decomposition of the EXAFS signals into a sum of several contributions, the n-body terms. It allows the direct comparison of the raw experimental data with a model theoretical signal. The procedure avoids any filtering of the data and allows a statistical analysis of the results. The theoretical signal is calculated ab initio and contains the relevant two-body $\gamma^{(2)}$, the three-body $\gamma^{(3)}$, and the four-body $\gamma^{(4)}$ multiple scattering (MS) terms. The two-body terms are associated with pairs of atoms, probing their distances and variances. The three-body terms are associated with triplets of atoms and probe angles, bond-bond, and bond-angle correlations. The four-body terms are associated to chains of four atoms, and probe distances and angles in between, and bond-bond and bond-angle correlations.

Data analysis is performed by minimizing a χ^2-like residual function that compares the theoretical signal, $\alpha_{mod}(E)$, to the experimental one, $\alpha_{exp}(E)$. In the case of the multiple edge fitting, the χ^2-like residual function is used to perform a simultaneous structural refinement over a selected number M of independent a-ray absorption spectra related to the same system:

$$R(\{\lambda\}) = \sum_{j=1}^{M} \sum_{i=1}^{N_j} \frac{[\alpha^i_{exp}(E_i) - \alpha^i_{mod}(E_i;\lambda_1,\lambda_2,\ldots,\lambda_p)]^2}{\sigma^2_{i,j}} \qquad (1)$$

where the index i runs over the number N_j of experimental energy points E_i of each absorption spectrum j. $\sigma^2_{i,j}$ is the variance associated with the $\alpha_{exp} - \alpha_{mod}$ random variable. In most cases $\sigma^2_{i,j}$ can be directly estimated from the experimental spectrum, and a k^m weighting (with $m = 2, 3, ...$) results in a good approximations. As in the usual single-edge case, the use of the equation specified above allows us to perform a statistical analysis of the structural results. The optimal best-fit values of the p parameters to be refined ($\lambda_1, \lambda_2, ..., \lambda_p$) along with their statistical error including correlation among different parameters can be evaluated as illustrated elsewhere.[32,46] Typical errors in the 0.001−0.01 Å range for the first neighbor bond distances have been found using such a ab initio multiple scattering calculation of the X-ray absorption cross section.

The phase shifts for the photoabsorber and backscatterer atoms were calculated ab initio starting from the structural model previously reported.[42] They were calculated according to the muffin-tin approximation and allowing for 10% overlap between the muffin-tin spheres. The Hedin−Lundqvist complex potential[47] was used for the exchange-correlation potential of the excited state. The core hole lifetime, Γ_c, was fixed to the tabulated value[48] and included in the phase shift calculation. The experimental resolution used in the fitting analysis was about 2 eV, in agreement with the stated value for the beam line used. The relevant E_0's values were found to be displaced by several eV with respect to the edge inflection point, and they are summarized in Table 2 together with the structural parameters. Concerning the amplitude correction factor S_0^2, we have performed a series of refinement processes of the XAFS signal for different S_0^2 (Fe), S_0^2 (Co), and S_0^2 (Ni) values chosen in an appropriate two-dimensional grid. A region of minima of the residual function was identified around S_0^2 (Fe) = 0.76(6), S_0^2 (Co) = 0.80(6), and S_0^2 (Ni) = 0.87(7). Structural refinements were performed using those values for the amplitude correction factor.

The fitting procedures at the Fe, Co, and Ni K-edge was conducted including the relevant set of multiple scattering paths that originates from the typical structure of hexacyanoferrates.[42] Hence, with the help of the Scheme 1, the theoretical signals included in the fitting procedures are (Fe K-edge) the two-atom contributions $\gamma_1^{(2)}$ Fe−C with degeneracy of 6, the three-body

(44) Filipponi, A.; Di Cicco, A.; Natoli, C. R. *Phys. Rev. B* **1995**, *52*, 15122.
(45) Filipponi, A.; Di Cicco, A. *Phys. Rev. B* **1995**, *52*, 15135.
(46) Filipponi, A. *J. Phys.: Condens. Matter* **1995**, *7*, 9343.
(47) Hedin, L.; Lundvquist, B. I. *J. Phys. C* **1971**, *4*, 2064.
(48) Krause, M.; Oliver, J. H. *J. Phys. Chem. Ref. Data* **1979**, *8*, 329.

Scheme 1

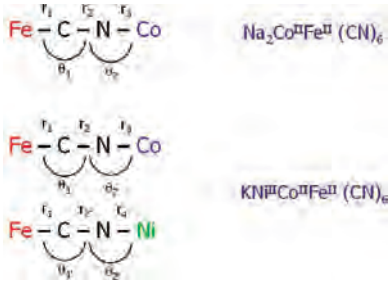

contribution $\eta_1^{(3)}$ Fe−C−N with degeneracy of 6, and the four body contribution $\eta_1^{(4)}$ Fe−C−N−Co with degeneracy of 6. It is worth noticing that the inclusion of the three-body term $\eta_1^{(3)}$ allows monitoring the shells beyond the first one by using the same three-atom coordinates both for the two-atom and the three-atom contributions. In fact, the three-body signal $\eta_1^{(3)}$ Fe−C−N includes both $\gamma^{(2)}$ Fe−N and $\gamma^{(3)}$ Fe−C−N contribution. Similarly, the $\eta_1^{(4)}$ MS signal includes two three body contribution, the $\gamma^{(3)}$ Fe−C···Co and the $\gamma^{(3)}$ Fe···N−Co and the interaction Fe···Co through the $\gamma^{(2)}$ Fe−Co signal. In addition, a $\gamma_1^{(2)}$ Fe−K(Na) signal, because of the contribution of the interstitial alkali cations, was considered as well. This contribution appears very weak but should be included altogether.

On the other hand, the signals associated to the Co K-edge that have been included in the fit are as follows: $\gamma_1^{(2)}$ Co−N with degeneracy of 4.5; $\eta_1^{(3)}$ Co−N−C with degeneracy of 4.5, and the $\eta_1^{(4)}$ Co−N−C−Fe with degeneracy of 4.5. Also, a second $\gamma^{(2)}$ signal, the $\gamma_2^{(2)}$ Co−O with degeneracy of 1.5 was necessary to take into account the "insoluble" structure of metal hexacyanoferrates [The inclusion of oxygen contribution in the first shell of Co as well as the unusual degeneracy of the MS signals here merits some details. The structure of hexacyanoferrates are related to the well-known "soluble" and "insoluble" forms [H.J. Buser, D. Schwarzenbach, W. Petter, A. Ludi, *Inorg. Chem.* **1977**, *16*, 2704]. In the "soluble" form a typical face-centered cubic structure $F\bar{4}3m$ is present, where Fe and Co ions are octahedrally coordinated by −CN and −NC groups, respectively. The structure of the "insoluble" forms also features a rigid cubic framework of linear chains −Fe−CN−Co− atoms (cubic cell $Pm\bar{3}m$), except that 1/4 of the $Fe(CN)_6^{4-}$ unit is vacant; with the empty nitrogen positions filled out by water molecules to complete the coordination shell of Co. Hence, Co atoms are present in this unit cell with three pseudosquare planar coordinated atom (CoN_4O_2) and one octahedrally coordinated Co atom (CoN_6), resulting in an average of $CoN_{4.5}O_{1.5}$. Measurements at the Fe K-edge are not affected by this issue, as every Fe atoms is coordinated octahedrally by six carbon.]. Certainly, in the case of the soluble primary structure, the first shell of cobalt is described by the $\gamma_1^{(2)}$ Co−N signal with a degeneracy of 6. In addition and in all cases, a $\gamma_3^{(2)}$ Co−K(Na) signal was included in the fitting procedure. In the same way, the signals associated to the Ni K-edge are the $\gamma_1^{(2)}$ Ni−N with degeneracy of 4.5, the $\gamma_2^{(2)}$ Ni−O with degeneracy of 1.5, $\gamma_3^{(2)}$ Ni−K(Na), the $\eta_1^{(3)}$ Ni−N−C with degeneracy of 4.5, and the $\eta_1^{(4)}$ Ni−N−C-Fe with degeneracy of 4.5. The selection of the "soluble" structural model is suggested by the stoichiometry data and from a fitting test as well. Besides, several fitting procedures on the compounds **II** and **III** were conducted. They were based on floating coordination numbers for $\gamma_1^{(2)}$ Co−N (N1) and $\gamma_2^{(2)}$ Co−O (N2) with the constraint of N1 + N2 = 6. Fits reported the results of 4.5(2) and 1.5(2) for N1 and N2, respectively, for both compounds considered. The numbers N1 and N2 become 5.5(3) and 0.5(3) in the case of compound **I**. Hence, these data coupled with stoichiometric data suggest a "soluble" primary structure for the compound **I** and an "insoluble" structure for compounds **II** and **III**. Notwithstanding, compound **I** has been analyzed considering a small fraction of "insoluble" structure as well.

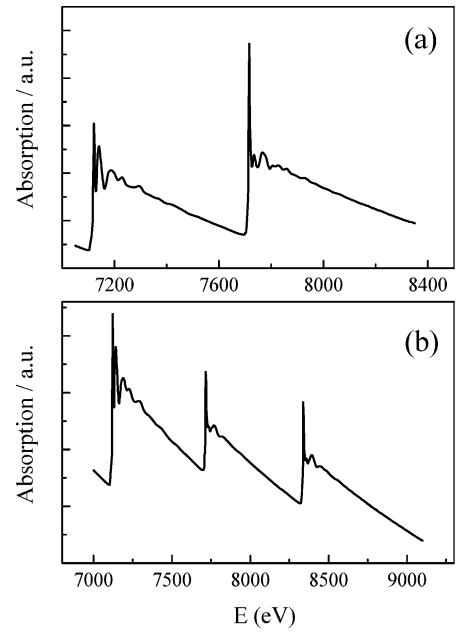

Figure 1. Experimental XAS data at the Fe and Co K-edge for compounds **I** (a) and **III** (b).

On the basis of this model, the total number of parameters included in the fitting procedure (including the structural and nonstructural terms E_0, S_0^2, and the experimental resolution) depend on the compounds investigated as well as on the chosen fitting strategy. The total number of parameters included in the fitting is found to be 24 (sample I and II) and 31 (sample III). The number of free parameters were 12 (sample I and II) and 18 (sample III). Besides, it is worth mentioning that in all cases the number of fitting parameters does not exceed the estimated "number of independent data points" $N_{ind} = (2\delta k \delta R/\pi) + 2$, ensuring that the fit is well determined and does not lead to parameters with very large errors, thus pointing out the reliability of the minimization.

Results and Discussion

Figure 1 shows the X-ray absorption spectra of compounds **I** and **III** (panels a and b). The two spectra are characterized by two or three close discontinuities due to the opening of absorption channels of metals of the investigated compounds: Fe, Co, and Ni. As their atomic number Z is progressive, that is, Z (Fe), $Z + 1$ (Co), and $Z + 2$ (Ni), they produce the typical effects of Figure 1b when the photon energy of the synchrotron radiation beam is scanned from the Fe K-edge energy to about 2000 eV. Let us consider the magnitude of the relative absorption edges (jump) of the three edges. Because the absorption process is sensitive to the metal concentration of a specimen (i.e., the actual density of the photoabsorber atom), the experimental jumps could provide a rough value of the relative metal concentration in our sample, as reported in Table 1. Data obtained from the XAS experimental spectra are close to those of the EDXF chemical analysis. Furthermore, the chemical analysis suggests the occurrence of the soluble form in compound **I**, and insoluble form in compound **II**and compound **III**.

As pointed out in the Introduction, the EXAFS spectrum of metal hexacyanoferrates is characterized by consistent MS effects, with a large four-body Fe−C−N-Co contribution. This, in turn, means that the second metal (Co while analyzing the Fe K-edge EXAFS spectrum, and vice-versa) contributes to the electron scattering processes. The Fe−C−N−Co atomic chain is simply described by a set of atoms vibrating around the equilibrium positions, whose structural parameters are indicated in the Scheme 1. Referring to cobalt hexacyanoferrate, the Co−N distance (r3) is reported to be essential in the definition of some chemical physical properties. For instance, it has been found to be a fingerprint of the spin transition of cobalt atom.[26–28] The Fe−C distance (r1) is found to be almost constant in metal hexacyanoferrates. Angles $\theta 1$ and $\theta 2$ define the linearity of the chain and are generally fixed at 180° (vibration from this equilibrium value are taken into account by the angle Debye−Waller factor). The CN bond interaction (r2) is particularly interesting because it is among the two metallic sites, and hence the r2 distance can be probed twice in the same Multiple Edge XAFS experiment. The strong Fe∼Co interaction is observable from both Fe and Co K-edge,[42] and appears in iron−copper bridged cyanide.[13] Data analysis allowing both edges to be probed simultaneously is called multiple-edge analysis and has been applied here using the GNXAS code program. The strong impact of the Multiple Edge approach in compounds characterized by multiple common pathways within the same molecule was identified since the first GNXAS application[13,14] on relatively simple compounds (one-common pathway). In this paper, the compounds investigated are characterized by multiple common pathways with the peculiar characteristic of sharing the entire structural parameters. Hence, the advantages of using the multiple edge approach are found to be enhanced. Another possibility is to consider the two edges separately: each EXAFS experimental spectrum is analyzed by using the same structural parameters, producing two sets of independent data.

The description of the structural parameters of mixed Co/Ni−Fe hexacyanoferrate is more complicated and appears in the Scheme 1 as well. In this case, two are the atomic linear chains to be probed in the same experiments, making the number of parameters almost double. This limits the accuracy of the structural determination in compound **III**. For instance, let us consider the estimation of the CN bond length. In this case the Fe atom sees two types of CN interactions, respectively linked to the Co and Ni, (r2 *and* r2′). Hence, we should admit less advantages of having three independent probes (Fe, Co, and Ni). Though, this limitation is compensated by the availability of a large number of experimental points that affects the Fe/Co/Ni multiple edge EXAFS spectrum of the Figure 1b.

Results of the different fitting procedures, which include the Multiple Edge and the Single Edge approaches, will be presented separately for the sake of clarity.

Multiple-Edge EXAFS Data Analysis. Figure 2 reports the best fit results (case of multiple-edge fit) for the three compounds investigated. The upper panels display the comparison of the experimental and theoretical EXAFS signals, whereas the corresponding Fourier Transforms (FTs) are shown in the lower panels. It is worth noticing that the Ni edge occurs only in sample **III**. The figure reveals that the theoretical curves match well with the experimental ones in all panels, indicating the reliability of the chosen structural model[42] and the accuracy of the data analysis.

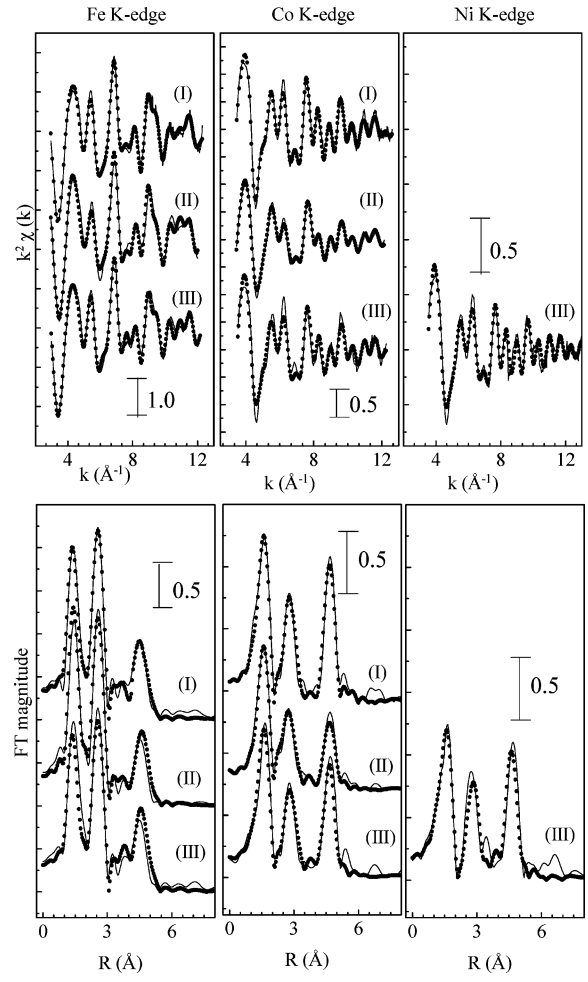

Figure 2. Comparison of the experimental (solid line) and theoretical (dotted line) k^2-weighted EXAFS signals for compounds **I**, **II**, and **III** at different metal K-edges (upper panels); corresponding FT k^2-weighted EXAFS signals are showed in lower panel.

An example of a best-fit result (compound **III**) in terms of single MS contributions is reported in Figure 3. Each panel of the figure corresponds to the different metal K-edges and shows the various contributions to the total theoretical signal and the comparison of the theoretical to the experimental one, at the bottom. This plot underlines the two peculiarities of the present data analysis: the large contribution of the three- and four body signals, whose intensities are comparable to the first shell signal, and the proper account of the atomic background because it is affected by the contributions due to the previous edge. For instance, as indicated in the figure, the $\gamma_1^{(2)}$ Fe−C (Fe) signal presents a continuation to the Co and Ni K-edge. The effect of the proper account of continuation of the XAFS signal of previous edges has been studied in the literature[12] showing very relevant effects while studying contiguous L edges.

A list of structural and nonstructural parameters obtained from the fitting procedure is presented in Table 2, together

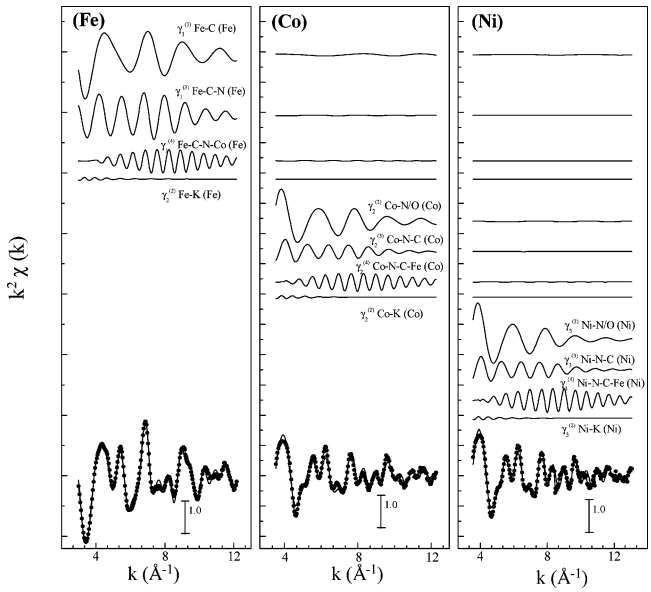

Figure 3. Details of the EXAFS analysis of the Fe, Co, and Ni K-edge of the sample **III**. The figure shows the individual EXAFS contributions, in terms of two-, three-, and four-body signals, to the total theoretical one (see text for details). The plot also shows the proper account of continuation of the individual XAFS signal of previous edges: for instance, the $\gamma_1^{(2)}$ Fe−C (Fe) signal presents continuation to the Co and Ni K-edge. At the bottom, the comparison of the total theoretical signal (solid line) with the experimental (dotted line) is also illustrated for each panel.

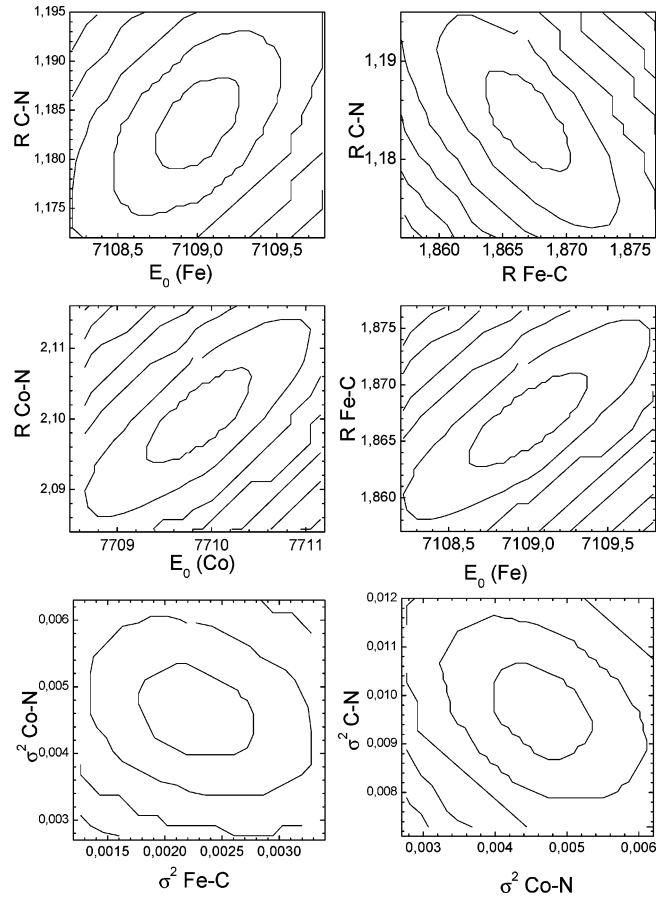

Figure 4. Examples of the two-dimensional section of the parameter space (contour plots) for sample I. These plots were selected among the parameters having strong correlation to reflect the highest error. The inner elliptical contour corresponds to the 95% confidence level.

with the associated errors. They were determined by the correlation maps (contour plot) for each pair of highly correlated parameters. Figure 4 shows the contour plots for compound **I**, as an example. These plots were selected among the parameters having strong correlation to reflect the highest error. The estimated statistical error[46] is associated with the 95% confidence interval. It is important to emphasize that this evaluation provides only statistical errors on EXAFS refined parameters, and it does not accounts for systematic errors [Systematic errors, which are introduced during both acquisition and analysis of EXAFS data, arise from a large number of sources. Sample inhomogeneities, radiation damage, thickness and particles size effect, insufficient suppression of higher harmonics, glitches, and improper sample alignment are examples of acquisition-related ones, whereas analysis-related errors include improper pre-edge subtractions and/or normalization, and improper determination of amplitude reduction factor. While the majority of systematic error may be eliminated following good data acquisition and analysis practices, others are unavoidable. Generally, statistical errors in EXAFS results from photon counting statistics, mechanical instabilities in the beamline, fluctuations in the position and intensity of the photon beam, and electronic noise.] in the theory or are peculiar to the experimental technique.

Table 2 indicates that the three Fe−C interatomic distances are similar, with values ranging from 1.866(4) for **I** to 1.890(8) Å for compound **II**. The slightly longer bond length of Fe−C in Fe^{III} with respect to Fe^{III} complexes has been recently pointed out by XAFS investigation of similar compounds in solid and solutions.[49] The C≡N bond lengths, ranging from 1.167(7) to 1.184(12) Å, are found to be in line with the values quoted for this class of compound[28,46] and more details will be discussed later. The Co−N interatomic distances are seen to be the same at around 2.09−2.10 Å regardless of the formal oxidation state of the Fe (sample **I** and **II**). This value agrees with those of mixed $Fe^{II}Co^{II}$ cyanides.[42,50] Also, the Co−N distance suggests no charge transfer event between Fe^{III} and Co^{II} in sample **II** (with the subsequent Co^{II} to Co^{III} oxidation) that also produces the well-known shortening of the Co−N interaction.[50] The phenomenon, not observed here, is due to a spin transition occurring at the Co site, making feasible the use of FeCo cyanides as magnetic devices.[28,50] The Co−O bond lengths are found to be closely the same (considering their associated errors) in all compounds and they agree with values normally quoted for cobalt complexes in similar environment[9,51] where the Co atom is coordinated with "mobile" water. EXAFS bond length variances associated with the bond lengths are almost the same, although values of compound **II** are lower than those of compound **I**.

(49) Hayakawa, K.; Hatada, K.; D'Angelo, P.; Della Longa, S.; Natoli, C. R.; Benfatto, M. *J. Am. Chem. Soc.* **2004**, *126*, 15618.
(50) Yokoyama, T.; Otha, T.; Sato, O.; Hashimoto, Y. *Phys. Rev B* **1998**, *58*, 8257.
(51) Giorgetti, M.; Berrettoni, M.; Ascone, I.; Zamponi, S.; Seeber, R.; Marassi, R. *Electrochim. Acta* **2000**, *45*, 4475.

Overall, the EXAFS analysis indicates that the Fe−C−N portion of the Fe−C−N−Co linear chain vibrates in the same manner around the equilibrium position for all compounds investigated. The addition over the single bond lengths of the −Fe−C−N−Co− structural units corresponds to $a/2$, where a is the cell parameter. The values obtained for the compounds **I**, **II**, and **III** agree within certain limit to the ones from powder XRD analysis, as shown in Table 2, thus underlying the reliability of the present analysis. In particular, as suggested by Zhang et al.,[14] it may be considered as an indicator of systematic error.

Single-Edge EXAFS Data Analysis. The single-edge EXAFS data analysis of Fe/Co/Ni hexacyanoferrates produces as much sets of independent structural parameters as the number of metals involved. Table 2 lists the corresponding structural and nonstructural parameters. The best fit results (plots of the experimental and theoretical EXAFS signals and of the corresponding Fourier transforms) of the compounds **I**−**II**−**III** are reported in Supporting Information, Figures S3−S6. The single edge refinements gave results that on average were of the same quality as those from the multiple-edge fits. In fact, although some differences on the quotation of the Fe−C, C≡N, and Co−N bond distances were evidenced, the average value of the Fe—Co distance in the linear chain is the same and close to the crystallographic value. On the contrary, a discrepancy is seen for an Fe single edge fit of sample **II**.

It is clear by examining the results of the isolated Fe and Co fits that the Fe−C bond essentially does not contribute to the Co edge and vice versa. Hence, the corresponding σ^2 Fe−C values are higher. In fact, the σ^2 Fe−C values for compounds **I**, **II**, and **III** (single edge fits) are found to be higher than those of the corresponding multiple edge fits. In addition, some pair distances are quoted different in the single edge case with respect to the multiple edge one. This is the case of the Co−N distance (Fe K-edge) of the compound **II** that is quoted 2.04 Å, that is, 0.05 Å shorter than the corresponding value of the multiple edge approach. The difficulty of determining the M(Co, Ni)−N interaction from the Fe K-edge is quite dramatic in the case of compounds **III**. This is evidenced from the obtained C≡N and Ni−N bond length in the single edge fits, also leading to odd values of the corresponding Fe−C bond distance.

It is important to remark here that the multiple edge approach overcome both problems of the "apparent" higher values of the σ^2's and of the unusual values of the C≡N or Ni−N distances. This is due to the advantages of using the multiple edge approach in this class of compounds, where all the structural parameters are fully correlated and a large number of useful experimental points allows a more accurate extraction of the structural parameters. In addition, the statistical errors associated to some parameters turn out to be reduced while using the multiple edge approach, as confirmed by the Fe−C and C≡N error values. This does not necessarily means that the fit errors, defined in the Experimental Section, are certainly reduced. In fact as reported in Table 2, the χ^2 like residual function of the single edge fits becomes lower in some cases (and higher in others). Though, the χ^2 like residual function of sample **III** become 35 times higher in the case of a Ni single edge fit with respect to the multiple edge case.

On the Determination of the CN Bond Length. Besides the fact that C≡N bond lengths (multiple edge approach) are found to be in line with the values quoted for this class of compound, we found differences in this bond length quotation while comparing different fitting strategies. This is the case of compounds **I** and **II**, as Table 2 reveals. First, the single edge approach at the Co K-edge is likely to underestimate this value, and the opposite is valid while considering the Fe K-edge. As a matter of fact, the values of the single edge approaches are still acceptable, considering the relative errors associated to the bond distance. For instance, the value of 1.183(5) Å for compound **I** (multiple edge fit) includes both 1.192(6) and 1.176(10) obtained at the Fe or Co K-edge only, even though the mean value of the bond length distribution is different. Second, the statistical error associated with bond lengths are smallest in the multiple edge case. In fact, values of 0.0005 and 0.0007 Å are found for compound **I** and **II**, respectively, that become twice in the case of single-edge (Co edge, compound **I** or Fe edge, compound **II**).

The compound **III** results also demonstrate the difficulty of determining a consistent C≡N bond distance when a the triple probe (Fe, Co, Ni) is considered. The various single edge approaches produce very different result whereas the multiple edge outcome agrees with the literature. In addition, the C≡N bond distances are quoted with errors that are found to be twice in comparison to those of compound **I** and **II**. These limitations have two main reasons. First, the fitting procedure is actually probing two different structural unit, namely, the −Fe−CN−Co− and the Fe−CN−Ni− and hence the C≡N bond distance parameter refers to two different chemical environments. This affects especially the errors of the selected structural parameter. The second limitation belongs to the single edge approaches versus the multiple edge one: the use of the multiple edge approach is making the three experiments to be considered as dependent, and optimizes to values intermediate between the three conditions.

Because of the above issues and considering the soluble/insoluble primary structure characteristics, compound **I** (multiple edge analysis) is the most reliable structural model for the measure of the CN bond length with EXAFS.

Conclusions

This work presents the potentiality of the EXAFS spectroscopy which, taking advantage of modern experimental and data analysis techniques, allows a detailed study of the structural properties of metal hexacyanoferrates. The first example of a multiple edge approach concerning three contiguous metal edges, on compounds with the peculiar characteristic of sharing the entire structural parameters, is given. The investigated samples are structurally characterized by several repeating, and planar, −Fe−CN−Co(Ni)− structural units. This particular structure permits double probe XAFS and highly efficient MS effects. The double probe

has allowed extending the number of experimental data to about 800 in compounds **I** and **II** and to about 1200 in compound **III**. This strongly affects the reliability of the data analysis because the same structural model is probed using larger number of experimental data (see Supporting Information, Scheme S1).

The XAS data analysis has been conducted taking into account the MS formalism, which represents the best approach as demonstrated several times since the pioneering work by Lee and Pendry[52] and further developed for the EXAFS case by the work of Natoli, Benfatto and coworkers.[53,54] The multiple scattering approach here produces large structural effect in the EXAFS spectrum of the selected compounds because of the large number of atomic Fe−C−N−Co/Ni linear chains characterizing the compounds.

The particular atomic arrangement of the cobalt hexacyanoferrate that are characterized by an almost perfect Fe−C−N−Co linear chain, a short distance between the two metal center, and a high degeneracy of the chains allowed monitoring the C≡N bond length with an unusual precision even though C or N are not the photoabsorbing atoms of the XAFS experiment.

Acknowledgment. Measurements at Daresbury Laboratory were supported by the European Community - Research Infrastructure Action under the FP6 "Structuring the European Research Area" Programme (through the Integrated Infrastructure Initiative "Integrating Activity on Synchrotron and Free Electron Laser Science").

Supporting Information Available: XANES spectra at the Fe and Co K-edges of compound **II**; fitting analysis (single edge approach) of the investigated samples; scheme of the experimental data points in multiple edge fitting analysis (7 pages, PDF). This material is available free of charge via the Internet at http://pubs.acs.org.

IC800289C

(52) Lee, P. A.; Pendry, J. B. *Phys. Rev. B* **1975**, *11*, 2795.
(53) Benfatto, M.; Natoli, C. R.; Bianconi, A.; Garcia, J.; Marcelli, A.; Fanfoni, M.; Davoli, I. *Phys. Rev. B* **1986**, *34*, 5774.
(54) Brouder, C.; Ruiz-Lòpez, M. F.; Pettifer, R. F.; Benfatto, M.; Natoli, C. R. *Phys. Rev. B* **1989**, *39*, 1488.